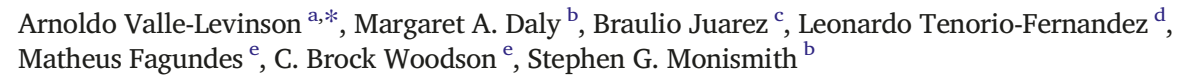
Contents lists available at ScienceDirect

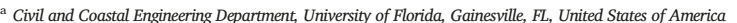
Science of the Total Environment

journal homepage: www.elsevier.com/locate/scitotenv



Influence of kelp forests on flow around headlands





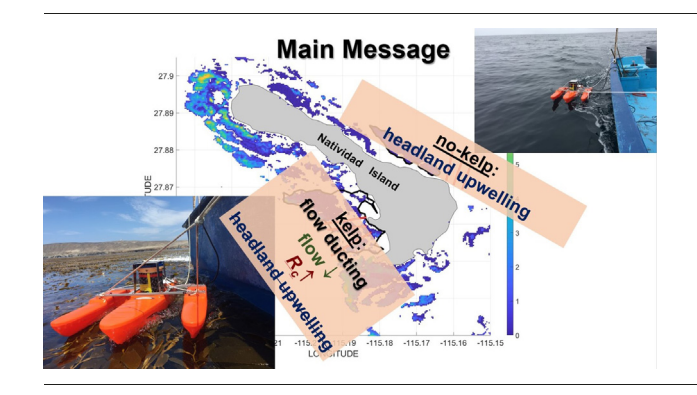
- b Department of Civil and Environmental Engineering, Stanford University, Palo Alto, CA, United States of America
- ^c Instituto de Investigaciones Oceanológicas, Universidad Autónoma de Baja California, Baja California, Mexico
- d Centro Interdisciplinario de Ciencias Marinas, La Paz, Baja California Sur, Mexico
- ^e School of Environmental, Civil, Agricultural, and Mechanical Engineering, University of Georgia, Athens, GA, United States of America

HIGHLIGHTS

· Dense kelp forests attenuate ambient flows, increasing their effective radius of curvature

- Dense kelp forests suppress headland upwelling.
- · Dense kelp forests promote flow ducting.

GRAPHICAL ABSTRACT



ARTICLE INFO

Article history: Received 27 August 2021 Received in revised form 11 January 2022 Accepted 13 February 2022 Available online 18 February 2022

Editor: Martin Drews

Keywords: Headland upwelling Flow ducting by kelp Flow attenuation by kelp Upwelling suppression by kelp

ABSTRACT

Kelp forests affect coastal circulation but their influence on upwelling around headlands is poorly understood. Tidalcycle surveys off two headlands with contrasting kelp coverage illustrated the influence of kelp forests on headland upwelling. Underway acoustic Doppler current and backscatter profiles were collected simultaneously to surface water temperature. Surveys occurred along three off-headland transects in July 25-29, 2018, off Isla Natividad, located midway on the western coast of the Baja California peninsula. Flows and water temperature distributions off the headland with no kelp coverage were consistent with headland upwelling. In contrast, the kelp around the headland with dense coverage: 1) attenuated the ambient flow; 2) favored an increase in effective radius of flow curvature; 3) promoted flow ducting, which consists of enhancing flow through channels unobstructed by kelp; and 4) suppressed headland upwelling. Kelp suppressed upwelling by channeling the flow away from the headland, keeping nearshore waters warmer than offshore

Plain language abstract: This study documents a way in which biology can affect physics in coastal ocean environments. In particular, the study describes how a kelp forest suppresses the upward pumping of cool subsurface waters that is typically found around headlands. Such suppression of subsurface waters injection occurs via a process that we refer to as 'flow ducting.' In flow ducting, coastal flows are channelized through kelp gaps, concentrated in bands <30 m wide, and kept away from the morphological influences of a headland. This ducting is analogous to the tortuous flow through porous media.

1. Introduction

Flow around headlands or points can produce localized upwelling (e.g., Figueroa and Moffat, 2000; Aiken et al., 2008), hereafter referred to

Corresponding author. E-mail address: arnoldo@ufl.edu (A. Valle-Levinson).





as 'headland upwelling.' Some of the consequences of headland upwelling are localized cooler surface waters and enhanced primary productivity around the headland. Headland upwelling is linked to secondary or transverse flows (e.g., Geyer, 1993; Pattiaratchi et al., 1987), which can be explained with cross-stream dynamics. In turn, cross-stream dynamics are related to streamwise flows through centrifugal accelerations, as these are proportional to the square of streamwise flows (e.g., Hench et al., 2002; Hench and Luettich, 2003; McCabe et al., 2009).

Streamwise flows moving around a headland or coastline point, result in a) streamwise flow acceleration, and b) an increase in centrifugal acceleration as flows separate from the headland (e.g., McCabe and MacCready, 2006; Stansby et al., 2016). Streamwise flow acceleration occurs within the radius of curvature of the headland and causes a drop in surface elevation. This drop in elevation represents an offshore pressure gradient, and is analogous to Bernoulli's principle of rapid flow causing low pressure. Dynamically, and in the cross-stream direction, the increase in centrifugal acceleration is balanced at the surface by the elevation slope (pressure gradient). However, this dynamic balance at the surface changes with depth as the streamwise flow decreases, because of bottom friction, together with the centrifugal acceleration. The cross-stream pressure gradient is depthindependent in such a way that there is a near-bottom imbalance in favor of the pressure gradient. This imbalance supports a sub-surface flow toward the headland, eventually upwelling when impinging on the coast. Headland upwelling is localized, concentrated within the radius of coastline or flow curvature, and expected along coastlines with enough bend to cause streamwise flow accelerations. Headland upwelling is similar to flows around meandering channels, where the secondary circulation drives upwelling off the inner bend of the meander (e.g., Hey and Thorne, 1974).

Along coastal temperate regions, and particularly off Eastern Boundary Currents (e.g., Benguela, Humboldt, Azores and California currents), kelp forests are common. These forests are known to attenuate waves and increase form drag on flow (Gaylord et al., 2007; Rosman et al., 2013). Overall, wind-waves and currents are expected to weaken over areas covered by kelp forests. These effects on hydrodynamics in turn influence ecosystem functions including larval dispersal, dissolved oxygen concentrations, pH values, and nutrient uptake (Jackson, 1977; Jackson and Winant, 1983; Fram et al., 2008; Gaylord et al., 2007). Flow attenuation by kelp forests in the vicinity of headlands should hypothetically suppress headland upwelling.

The objective of this study is to test this hypothesis by determining whether kelp forests that appear off a headland indeed hinder headland upwelling. To do so, underway current velocity profiles and surface water temperature were collected off two headlands, one with dispersed kelp coverage, and one with dense kelp coverage. The study was performed on Isla Natividad, found off Punta Eugenia, the most prominent point in the middle of the western coast of the Baja California peninsula (Fig. 1a), near the southernmost limit of the California Current.

2. Methods

To test the hypothesis that kelp forests suppress headland upwelling, data were collected over two headlands at either side of Isla Natividad (Fig. 1b). The sampling strategy consisted of three offshore transects around headlands on the eastern (1E, 2E, 3E) and western (1W, 2W, 3W) coast of the island. Both headlands were located over the southern half of the island (Fig. 1b) but only the western headland had dense kelp (*Macrocyctis pyrifera*) forests around it. The objective of the sampling strategy was to capture variations of the flow around the headland throughout full tidal cycles. Because the study area is dominated by mixed tides with semidiurnal dominance, sampling was designed to cover at least one 25-hr cycle. This strategy also allowed separation of tidal and residual or subtidal signals (e.g., Valle-Levinson and Atkinson, 1999) to identify flow fields typical of headland upwelling. Wind conditions should be sufficiently weak (<7–8 m/s) to allow towed-ADCP data collection.

Each transect was covered by Acoustic Doppler Current (ADCP) profiles of water velocity, acoustic backscatter, and values of surface water temperature. Raw data were recorded at 2 Hz while the ADCP was towed on a catamaran on the side of a boat from the local fisher cooperative. Acceptable data were trimmed to allow 3-beam solution values with >70% good and <100 $\rm m^2/s$ transport. On the east side of the island, transects were traversed at $\sim\!2$ m/s over waters with minimal kelp presence. East-side transects were covered on July 25th, 2018, for 12 h, because of an emergency for the fishing cooperative, and then re-occupied from July 26 to July 27, 2018. Transects on the west side were sampled over dense kelp forests (see photo on Fig. 1b). Sampling was executed interruptedly, again because of cooperative emergencies, from July 28th to July 29th, 2018. Wind conditions during ADCP sampling averaged <3 m/s, according to data from a station 20 km away, at Cedros Island.

The survey on the east side of the island extended mainly over three transects around a headland. Transect 1E was a few tens of meters to the west of the headland, while 2E and 3E were to the east. Sampling covered one full diurnal tidal cycle with ensembles of 25 velocity profiles and temperature values. Boat and ADCP speeds of 2 m/s on the east side represented ensembles of ~12.5 s (i.e., 25 profiles) with a spatial resolution of 25 m. Surface water temperature and velocities were used to construct Hovmöller or phase diagrams (along-transect distance vs time) that provided information on the offshore temperature structure and its variation with time at each of the three transects. These diagrams provided the first diagnosis for headland upwelling. Typical data processing (e.g., Valle-Levinson and Atkinson, 1999) was followed to obtain the vertical structure of tidal residual currents along each of the three transects. Residual flow contours provided a second diagnostic for headland upwelling.

On the west side of the island, in contrast, transects were mostly sampled over kelp forests and had a similar spatial extent as on the east side. Data were collected while towing at mean speeds of ~ 1 m/s, slower than on the east side because of the kelp density. Transducer pairs in the ADCP were nearly perpendicular and parallel to flow direction, allowing resolution of gaps in kelp. Water velocity and backscatter profiles were used to identify the predominant direction and vertical structure of overall currents in the region sampled. This was done with 80-profile ensembles for a horizontal resolution of ~40 m. Data coverage of <12 continuous hours precluded separation of tidal residual currents from tidal currents. Furthermore, all data were processed to achieve a spatial resolution of 4 m by averaging 8 profiles. Surface temperature values and ~40-m resolution surface velocities were also arranged in Hovmöller diagrams to diagnose headland upwelling. Surface velocity data with 4-m resolution resulted in noisy phase diagrams because of flow ducting through kelp, as explained in Results and Discussion.

On the west side, backscatter profiles with 4-m horizontal resolution were also used as proxy for kelp presence. Backscatter signals helped detect kelp grouping and their effect on flows. Backscatter profiles B(z,t) were collapsed into absolute values of depth-averaged anomalies |I|. |I| was calculated by vertically averaging B(z,t) to obtain $B_a(t)$. B_a was transformed, following Pleuddemann and Pinkel (1989), and Rippeth and Simpson (1998), to $B_t(t) = 10 \log(B_a)$. Finally, |I| was calculated at each time from the absolute value of $|B_t - B_t|$, where $|B_t|$ is a horizontal low-pass filtered version of $|B_t|$ centered, arbitrarily, at 40 m. This horizontal filtering eliminated the trend in backscatter observed from the beginning to the end of each transect repetition. Gaps in |I| at the surface remained practically depth-independent, suggesting a reliable representation of kelp fronds.

3. Results

3.1. East-side headland (scarce kelp coverage)

Phase diagrams of surface flow and temperature (Fig. 2a, b, c) and cross-sections of residual flows (Fig. 3a, b, c) show evidence of headland upwelling. Surface temperature increased offshore at the three transects during the times when the streamwise flows were strongest, i.e., most markedly around July 26.8. These features were more evident over transects 2E and 3E than on 1E as they were around and downstream of the headland, whereas 1E was just upstream of the headland. In transect 1E, streamwise

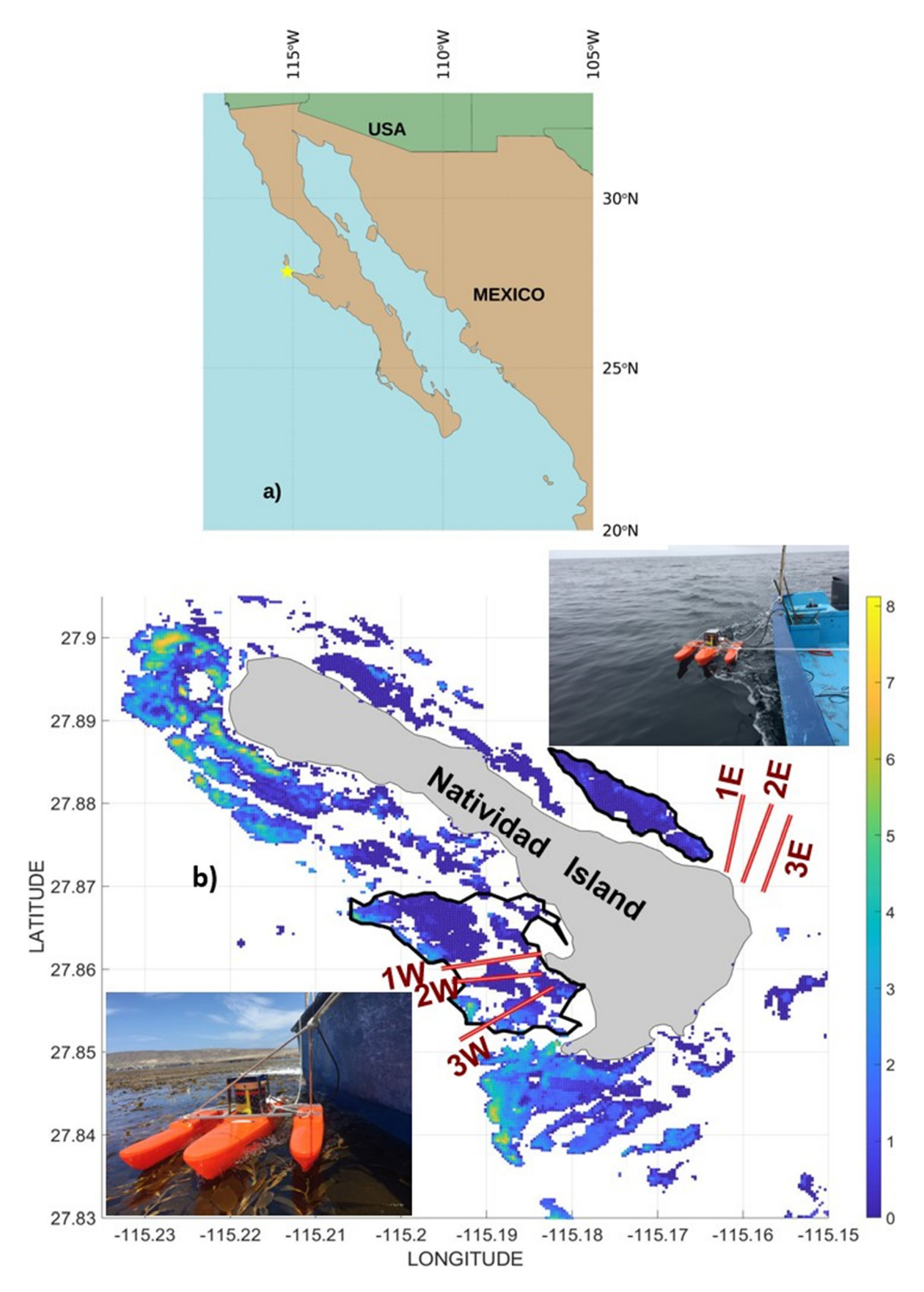


Fig. 1. Study site over the east and west side of Natividad Island, which is placed in a regional context as the yellow star on a). Sampling transects appear on b) with corresponding kelp coverage (color contours in relative units) and photographs of ADCP towing conditions, illustrating the kelp forest on the west side (1W, 2W, 3W). Regional flow direction was southeastward during sampling. Black contours on b) delineate dense kelp forests in proximity of sampling. Kelp coverage data courtesy of Tom Bell (UCSB).

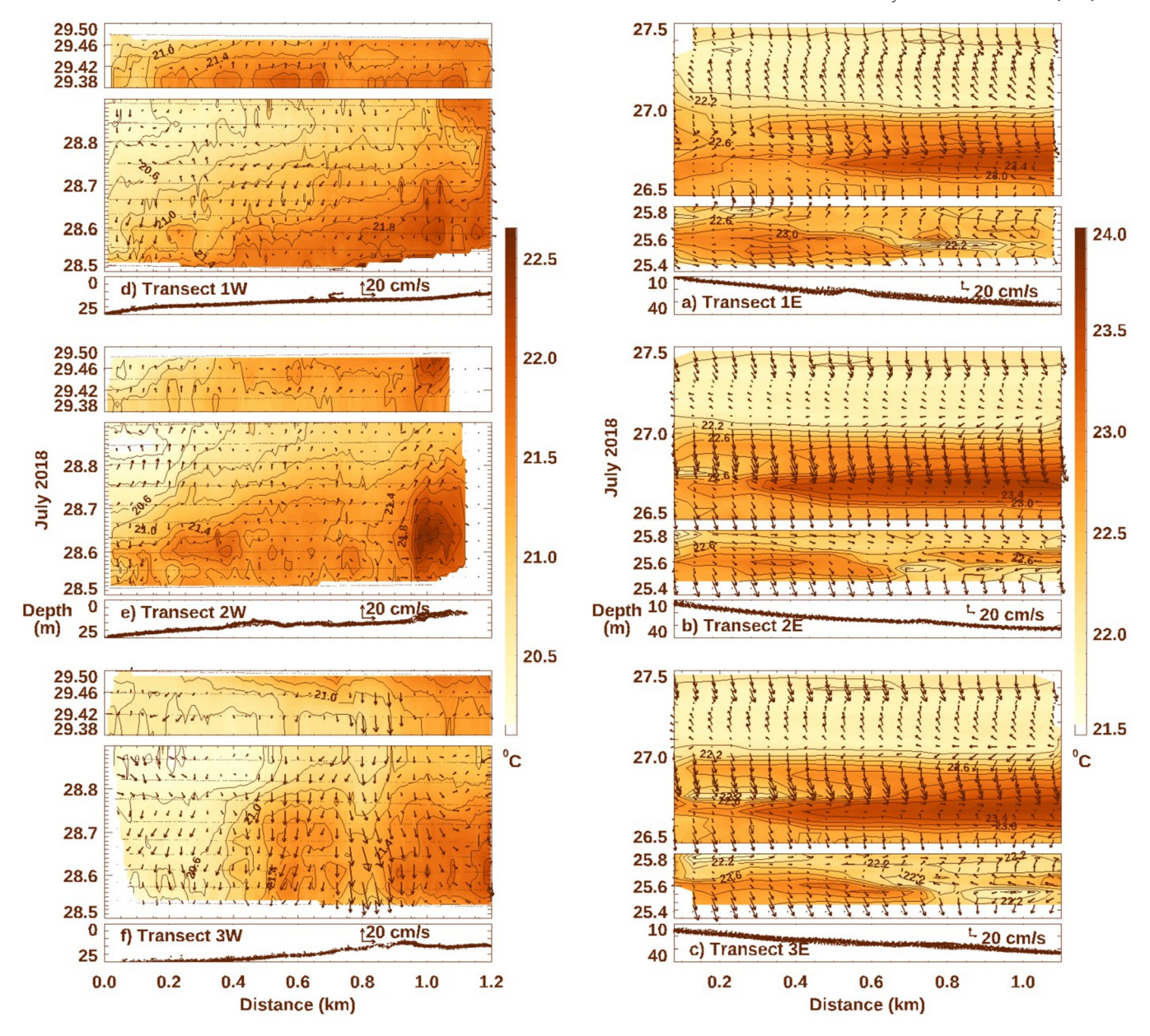


Fig. 2. Surface properties over the west and east side of Natividad Island. Panels a), b) and c) (on the right) show phase diagrams of surface temperature (in color) and velocity vectors on the east of the island. Vertical axes display day in July 2018. The gap between 25.8 and 26.5 indicates an interruption in the surveys. Panels with labels exhibit the bathymetric profile of each transect. Panels d), e), f) (on the left) show phase diagrams of surface temperatures, velocity vectors and bathymetric profiles on the west side of the island. Visible, tightly spaced, dots on these panels represent time and position of measurements.

flows were weaker than at the other two and were deflected offshore in the proximity of the headland (Fig. 2a–c). The relatively lower temperature and the modified flow fields developed as the flow was moving around the headland, indicative of headland upwelling manifestations near the airwater interface.

Cross-sections of the mean flow off the east-side headland further suggested localized headland upwelling. The streamwise flow component (colored contours in Fig. 3a, b, c) was dominated by southeastward flow in Transects 2E and 3E that weakened at the surface in Transect 1E as the mean flow sorted its way around the headland, and even reversed direction in the lower layer. In the stream-normal component (arrows in Fig. 3a, b, c), the three transects described typical secondary circulation conditions. Offshore residual flow appeared consistently near the surface out to $\sim\!600$ m from the transect origin. Onshore flow centered at a depth of $\sim\!10$ m (Fig. 3a, c), and developed most robustly between 200 and 600 m from the transects' origin.

3.2. West-side headland (dense kelp coverage)

Off the west-side headland, surface water temperature consistently decreased offshore over the three transects (Fig. 2d, e, f). This onshore increase in surface water temperature was contrary to expectations from headland upwelling despite the headland being more prominent than the one on the east side. Surface water temperature distributions in space and time suggested that some mechanism was suppressing headland upwelling on this side of the island. Surface flow fields were much more incoherent from transect to transect on the west side than on the east side of the island. This heterogeneity was likely because of kelp influence on the flow.

Effects of kelp coverage on flow fields over the west side were only suggestive with smoothed fields, i.e., 80-profile ensembles with $\sim\!40$ m resolution. These fields (Fig. 3d through h) displayed bands of enhanced flow magnitude that were $100{-}200$ m wide. Banding was attributed to blockage or attenuation by apparent obstacles, likely kelp forests. However, there

(one transect) Constant of the properties of th

Distance From Origin (km)

Tidally Evolving Flow Fields West Side

Tidal Residual Flow Fields East Side (three transects)

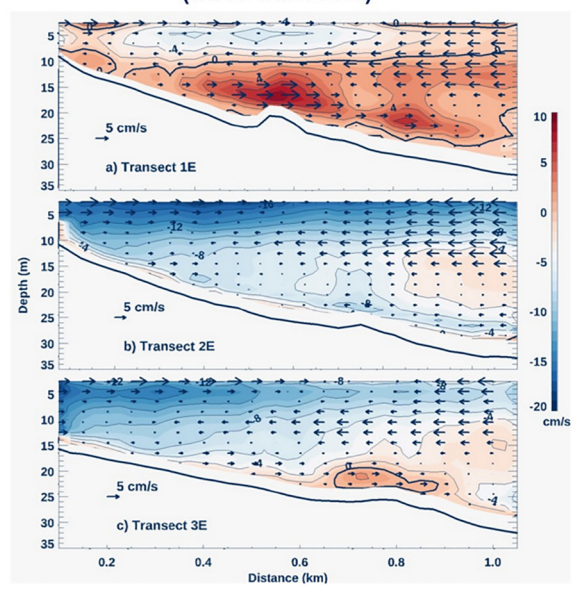


Fig. 3. Cross-sections (distance from shore vs depth) of residual flows on the east side of the island and tidally evolving flows on the west side. Residual flows [a), b) and c)] display along-shelf flow (in color) and cross-shelf flow (as vectors). Transects 1E, 2E and 3E refer to those labeled on Fig. 1b. Shore is on the left. Positive along-shelf flow is away from the viewer and vectors toward the right represent offshore flows. Continuous thick lines indicate bottom profiles with corresponding masking of side-lobe effects on velocity fields. Panels d) through h) indicate 80-profile ensembles of the along-shelf flow on the west side of the island, only for Transect 1W (as labeled on Fig. 1b), and at different tidal phases (as shown in the insert of d). The coast on these panels is on the right. As in panels a), b) and c), blue contours indicate flows toward the viewer.

was no clear correspondence between smooth flow and |I|, an indicator of kelp presence (Fig. 3d through h). In addition to these bands of enhanced flow, the fields over transect 1W illustrated tidal variations and vertically sheared structures in the streamwise flow. The vertically sheared structure was inhomogeneous along the transect, likely from spatially varying drag on the flow. Moreover, these smoothed fields provided a larger scale context to the fine scale (\sim 4 m) flow fields that explain the hindrance of headland upwelling off the west-side headland.

Effects of kelp coverage on flows were most evident with the high horizontal resolution (~4 m) data (Fig. 4). Velocity fields seem to have been ducted between kelp plants as indicated by dark-blue vertical banding in the along-shelf flow (Fig. 4). This banding showed spatial scales between 10 and 30 m. Moreover, flows off the west kelp-covered headland were overall weaker (max of 0.3 m/s) than off the east uncovered headland (over 0.5 m/s). Peaks in |I|, representing most kelp coverage, were associated with narrow bands (between 20 and 30 m wide) of hampered flows, or flow ducting between kelp. Ducting on transect 1W (Fig. 4) was only evident when the surface flow was southward (negative or blue contours in Fig. 3). Transect 1W was near the northern edge of the kelp forest sampled, so when the surface flow was northward (bottom two panels on Fig. 4), the flow at transect 1W was already ducted by upstream kelp coverage (to the south) of the transect. Because of this flow ducting at different portions of the kelp forest, the ambient streamwise flow was isolated from morphologic influences from the coastline thus hindering headland upwelling (Figs. 2, 3, 4).

4. Discussion

Observations near a headland on the east side of Isla Natividad provided evidence for headland upwelling in both, instantaneous surface properties and in cross-sections of mean flows (Figs. 2 and 3). This headland upwelling has been shown to be linked to flow separation at horizontal scales of the headland scale, usually defined by its radius of curvature, R. Thus, headland upwelling strength would be linked to centrifugal acceleration, U_s^2/R , which is connected to the streamwise flow U_s . Although the west-side headland has smaller radius of curvature R than the east-side headland, the local

or effective radius of curvature becomes larger due to kelp presence and *flow ducting*. In addition, kelp coverage attenuates ambient flows U_s that further reduces centrifugal accelerations.

Kelp coverage off a headland has four immediate effects on headlandrelated flows: attenuation of ambient flows; increase of effective radius of curvature; stimulation of flow ducting; and suppression of headland upwelling. Because of flow ducting through a complex network of kelp plants, it is hypothesized that flows should be channelized through tortuous, ductlike paths within a kelp forest. Conceptually similar to preferential flow in porous media (Simunek et al., 2003), flow ducting in kelp forests results in highly irregular flow patterns. Most kelp forest hydrodynamic experiments use bottom mounted ADCP's which are placed in open patches inside kelp forests to avoid interference by individual kelp plants (Gaylord et al., 2007; Rosman et al., 2013). Therefore, the flows thus observed could be biased as higher than average by nature of the experimental design. Observational biases should be considered when modeling coastal flows and larval, nutrient, or pollutant dispersal in kelp forests. While flows entering kelp forests are attenuated and could cause reduced dispersion of dissolved and suspended material, flow ducting should actually increase dispersion (Nepf, 2012). Flow ducting should also provide localized sites of fertilization and nursey grounds (safe spaces) for various species.

In other coastlines with prominent headlands, it is possible that the wind stress varies around headlands (Winant et al., 1988; Winant and Dorman, 1997). A wind stress increase on one side of the headland may favor upwelling processes. In the particular case of Isla Natividad, the spatial scales of the island and of the headlands seem to be too small to produce spatial variability in the wind stress (Winant et al., 1988). Furthermore, theoretical results with spatially constant wind stress may produce upwelling around headlands (Winant, 2006). The observations off Isla Natividad, strongly suggest that the upwelling is hampered by kelp forests.

5. Conclusion

Observations around headlands with contrasting kelp coverage illustrated the influence of living organisms on coastal hydrodynamics. Observations indicated flow attenuation within a kelp forest and demonstrated

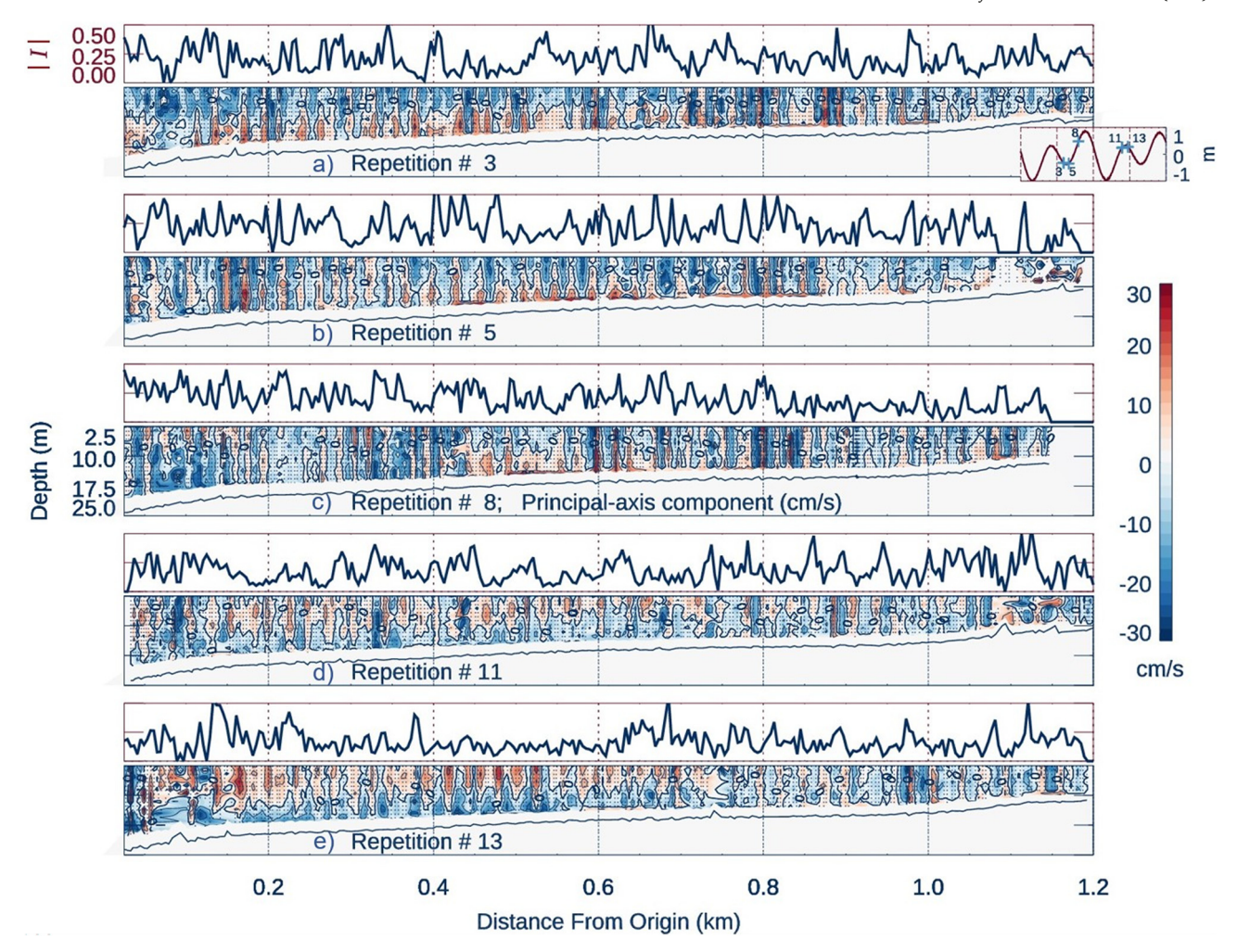


Fig. 4. Same cross-sections as in Fig. 3d through h, i.e., Transect 1W, but for data with 4-m resolution and with the proxy for kelp distribution |I|. Dots on each panel indicate position of data that met the trimming criteria described in Methods. Panels a) and b) illustrate surface flow going toward the viewer at the higher-low tide of the cycle. Panels d) and e) display opposite conditions at the lower-high tide of the cycle, with surface flow moving away from the viewer. Flow ducting is best documented in panels a) and b) as the transect is on the upstream side of the kelp forest, relative to the overall flow. Panels d) and e) display the same transect but on the downstream end, relative to the overall flow, of the kelp forest.

flow ducting through kelp forests. Flow ducting consists of mini-channels, $\sim\!\!10$ to 30 m wide, of relatively enhanced flow through kelp forests. Additionally, flow ducting increases the effective radius of curvature around a headland and prevents headland upwelling. Flow ducting may enhance the creation of safe spaces, having wide-reaching ecological implications.

Data and code availability

All data used for this manuscript may be obtained at "https://zenodo. org/record/5182648" (doi:https://doi.org/10.5281/zenodo.5182648).

CRediT authorship contribution statement

Arnoldo Valle-Levinson – designed experiment, collected and analyzed data, wrote manuscript.

Margaret A. Daly - designed experiment, edited manuscript.

Braulio Juarez - collected data, edited manuscript.

Leonardo Tenorio - collected data, edited manuscript.

Matheus Fagundes - edited manuscript.

 $C.\ Brock\ Woodson-designed\ experiment,\ edited\ manuscript.$

Stephen G. Monismith - designed experiment, edited manuscript.

Declaration of competing interest

The authors declare that they have no known competing financial interests or personal relationships that could have appeared to influence the work reported in this paper.

Acknowledgments

This study was funded by NSF project OCE-1736830, OCE-1737090. Members of the cooperative Buzos y Pescadores and the Isla Natividad community are gratefully acknowledged for their participation and support.

References

Aiken, C., Castillo, M., Navarrete, S., 2008. A simulation of Chilean Coastal Current and associated topographic upwelling near Valparaiso, Chile. Cont. Shelf Res. 28 (17), 2371–2381.

Figueroa, D., Moffat, C., 2000. On the influence of topography in the induction of coastal upwelling along the Chilean coast. Geophys. Res. Lett. 27, 3905–3908.

Fram, J.P., Stewart, H.L., Brzezinski, M.A., Gaylord, B., Reed, D.C., William, S.L., MacIntyre, S., 2008. Physical pathways and utilization of nitrate supply to the giant kelp, Macrocystis pyrifera. Limnol. Oceanogr. 53 (4), 1589–1603.

Gaylord, B., Rosman, J.H., Reed, D.C., Koseff, J.R., Fram, J., MacIntyre, S., Arkema, K., McDonald, C., Brzezinski, M.A., Largier, J.L., Monismith, S.G., Raimondi, P.T., Mardian, B., 2007. Spatial patterns of flow and their modification within and around a giant kelp forest. Limnol. Oceanogr. 52 (5), 1838–1852.

- Geyer, W.R., 1993. Three-dimensional tidal flow around headlands. J. Geophys. Res. 98 (C1), 955–966
- Hench, J.L., Luettich Jr., R.A., 2003. Transient tidal circulation and momentum balance at a shallow inlet. J. Phys. Oceanogr. 23, 913–932.
- Hench, J.L., Blanton, B.O., Luettich Jr., R.A., 2002. Lateral dynamic analysis and classification of barotropic tidal inlets. Cont. Shelf Res. 22, 2615–2631.
- Hey, R.D., Thorne, C.R., 1974. Secondary flows in river channels. Area 7 (3), 191–195.
- Jackson, G.A., 1977. Nutrients and production of giant kelp, Macrocystis pyrifera, off southern California. Limnol. Oceanogr. 22, 979–995.
- Jackson, G.A., Winant, C.D., 1983. Effect of a Kelp forest on coastal currents. Cont. Shelf Res. 2, 75–80.
- McCabe, R.M., MacCready, P., 2006. Form drag due to flow separation at a headland. J. Phys. Oceanogr. 36, 2136–2152.
- McCabe, R.M., MacCready, P., Hickey, B.M., 2009. Ebb-tide dynamics and spreading of a large river plume. J. Phys. Oceanogr. 29, 2839–2856.
- Nepf, H.M., 2012. Flow and transport in regions with aquatic vegetation. Annu. Rev. Fluid Mech. 44, 123–142.
- Pattiaratchi, C., James, A., Collins, M., 1987. Island wakes and headland eddies: a comparison between remotely sensed data and laboratory experiments. 92 (C1), 783–794.
- Pleuddemann, A.J., Pinkel, R., 1989. Characterization of the patterns of diel migration using a Doppler sonar. Deep-Sea Res. 36, 509–530.

- Rippeth, T.P., Simpson, J.H., 1998. Diurnal signals in vertical motions on the Hebridean Shelf. Limnol. Oceanogr. 43, 1690–1696.
- Rosman, J.H., Denny, M.W., Zeller, R.B., Monismith, S.G., Koseff, J.R., 2013. Interaction of waves and currents with kelp forests (*Macrocystis pyrifera*); insights from a dynamically scaled laboratory model. Limnol. Oceanogr. 58 (3), 790–802.
- Simunek, J., Jarvis, N., van Genuchten, M., Gardenas, A., 2003. Review and comparison of models for describing non-equilibrium and preferential flow and transport in the vadose zone. J. Hydrol. 272, 14–35.
- Stansby, P., Chini, N., Lloyd, P., 2016. Oscillatory flows around a headland by 3D modelling with hydrostatic pressure and implicit bed shear stress comparing with experiment and depth-averaged modelling. Coast. Eng. 116, 1–14.
- Valle-Levinson, A., Atkinson, L., 1999. Spatial gradients in the flow over an estuarine channel. Estuaries 22 (2A), 179–193.
- Winant, C.D., 2006. Three-dimensional wind-driven coastal circulation past a headland. J. Phys. Oceanogr. 36 (7), 1430–1438.
- Winant, C.D., Dorman, C.E., 1997. Seasonal patterns of surface wind stress and heat flux over the southern California bight. J. Geophys. Res. 102, 5641–5653.
- Winant, C.D., Dorman, C.E., Friehe, C.A., Beardsley, R.C., 1988. The marine layer off Northern California: An example of supercritical channel flow. J. Atmos. Sci. 45, 3588–3605.